

Formation of bright solitons and soliton trains in a fermion-fermion mixture by modulational instability

Sadhan K. Adhikari[‡]

Instituto de Física Teórica, UNESP – São Paulo State University, 01.405-900 São Paulo, São Paulo, Brazil

Abstract.

We employ a time-dependent mean-field-hydrodynamic model to study the generation of bright solitons in a degenerate fermion-fermion mixture in a cigar-shaped geometry using variational and numerical methods. Due to a strong Pauli-blocking repulsion among identical spin-polarized fermions at short distances there cannot be bright solitons for repulsive interspecies interactions. Employing a linear stability analysis we demonstrate the formation of stable solitons due to modulational instability of a constant-amplitude solution of the model equations for a sufficiently attractive interspecies interaction. We perform a numerical stability analysis of these solitons and also demonstrate the formation of soliton trains by jumping the effective interspecies interaction from repulsive to attractive. These fermionic solitons can be formed and studied in laboratory with present technology.

PACS numbers: 03.75.Ss, 05.45.Yv

[‡] Electronic address: adhikari@ift.unesp.br;
URL: <http://www.ift.unesp.br/users/adhikari/>

1. Introduction

After experimental observation and the study of bright solitons in Bose-Einstein condensates (BEC) [1–3], recent observations [4–7] and experimental [8–10] and theoretical [11–14] studies of a degenerate Fermi gas (DFG) by sympathetic cooling in the presence of a second boson or fermion component suggest the possibility of soliton formation [15] in a degenerate fermion-fermion mixture (DFFM). Apart from the observation of a DFG in the degenerate boson-fermion mixtures (DBFM) ${}^6,{}^7\text{Li}$ [6], ${}^{23}\text{Na}$ - ${}^6\text{Li}$ [7] and ${}^{87}\text{Rb}$ - ${}^{40}\text{K}$ [8,9], there have been studies of the following spin-polarized DFFM ${}^{40}\text{K}$ - ${}^{40}\text{K}$ [4] and ${}^6\text{Li}$ - ${}^6\text{Li}$ [5].

The dimensionless one-dimensional nonlinear Schrödinger (NLS) equation in the attractive (self-focussing) case [16]

$$i\frac{\partial\phi}{\partial t} + \frac{1}{2}\frac{\partial^2\phi}{\partial y^2} + |\phi|^2\phi = 0. \quad (1)$$

sustains the following bright soliton [16]:

$$\phi(y, t) = a \operatorname{sech}[a(y - vt)]e^{ivy - i(v^2 - a^2)t/2 + i\sigma} \quad (2)$$

The parameter a represents the amplitude as well as pulse width, v the velocity, and σ is a phase constant. These bright solitons are possible only in one dimension. In two and three dimensions they are allowed in the presence of a transverse trap [1, 15], or in the presence of an oscillating nonlinearity [17]. Apart from bright solitons in the attractive case, gap solitons are possible in the repulsive (self-defocussing) case in the presence of a periodic potential [18].

Bright solitons in a BEC are formed due to a nonlinear atomic attraction [1, 2]. As the interaction in a pure DFG at short distances is repulsive due to strong Pauli blocking, there cannot be bright solitons in a DFG. However, bright solitons can be formed [19, 20] in a DBFM in the presence of a sufficiently strong boson-fermion attraction which can overcome the Pauli repulsion among identical fermions. Bright solitons can also be formed in a binary mixture of repulsive bosons supported by interspecies attraction [21].

We demonstrate the formation of stable fermionic bright solitons in a DFFM for a sufficiently attractive interspecies interaction. In a DFFM, the coupled system can lower its energy by forming high density regions, the bright solitons, when the attraction between the two types of fermions is large enough to overcome the Pauli repulsion. We use a coupled time-dependent mean-field-hydrodynamic model for a DFFM and consider the formation of axially-free localized bright solitons in a quasi-one-dimensional cigar-shaped geometry using numerical and variational solutions. The present model is inspired by the success of a similar model used recently in the investigation of collapse [14, 22] and bright [20] and dark [23] solitons in a DBFM, and black solitons [24] and mixing-demixing [25] in a DFFM.

We study the condition of modulational instability of a constant-amplitude solution of the present model under a plane-wave perturbation and demonstrate the possibility of the formation of bright solitons by a linear stability analysis. We find that for

a sufficiently strong interspecies interaction, under the plane-wave perturbation the constant-amplitude solution becomes unstable and localized solitonic solutions may appear. We present a numerical stability analysis of these bright solitons by introducing different small perturbations when the solitons undergo stable and sustained breathing oscillation.

We also consider and study the formation of a soliton train in a DFFM by a large sudden jump in the interspecies fermion-fermion scattering length realized by manipulating a background magnetic field near a Feshbach resonance, experimentally observed in two hyperfine states of the following spin-polarized DFFMs: ${}^6\text{Li}$ - ${}^6\text{Li}$ and ${}^{40}\text{K}$ - ${}^{40}\text{K}$ [26]. This procedure effectively and rapidly turns a repulsive DFFM to a highly attractive one and generates bright solitons. An experimental realization of bright solitons in a DFFM could be tried in two hyperfine states in samples such as ${}^6\text{Li}$ - ${}^6\text{Li}$ or ${}^{40}\text{K}$ - ${}^{40}\text{K}$ using a Feshbach resonance. However, there is already experimental evidence [27] and theoretical conjecture [28] that the maximum attractive force, that can be created by a Feshbach resonance in fermionic atoms in two hyperfine states is limited by quantum mechanical constraints of unitarity. Although there is a limit to the creation of attraction in a two-component spin-polarized DFFM in two hyperfine states, there is no such limit in a multi-component spin-polarized DFFM [29] or a DFFM composed of atoms of distinct mass [30]. So, if bright solitons and soliton trains cannot be efficiently created in a two-component DFFM in two hyperfine states, a better and more efficient DFFM for the creation of solitons could be the mixture of fermionic atoms of distinct mass, where one can avoid the problem of a possible suppression of interspecies attraction. One such system, among many others, could be the mixture of spin-polarized ${}^6\text{Li}$ - ${}^{40}\text{K}$ mixture: both ${}^6\text{Li}$ [5, 31] and ${}^{40}\text{K}$ [4] have been trapped and studied in laboratory. The formation of bright solitons in a DFFM by turning the effective interspecies interaction among spin-polarized fermions from repulsion to strong attraction seems within the reach of present experimental possibilities.

Here we shall be interested in the formation of bright solitons in a spin-polarized DFFM of different fermionic atoms in the presence of strong interspecies attraction and we shall ignore the possibility of the formation of a Bardeen-Cooper-Schreiffer (BCS) condensate [32] through Cooper pairing. A BCS condensate is usually formed in the presence of a weak attraction among identical fermions with fermion pairs in the singlet (spin parallel) state. The formation of a BCS condensate should not be favored in a spin-polarized (spin antiparallel) two-component DFFM with strong attraction among the different types of atoms, as a strong interspecies attraction is not the domain of BCS condensation. By choosing a strong interspecies attraction our study stays in the BEC region of the BCS-Bose crossover problem [33] strongly favoring molecule formation. The solitons once formed will decay via molecule formation of two different types of fermionic atoms [34] as in the case of bosonic solitons. Nevertheless, such molecule formation is a slow process and can be accounted for by a three-body recombination term as introduced in a previous study of collapse in a DFFM [35]. The molecule formation will eventually destroy the solitons in the DFFM, albeit, at a slow rate. The

same is true in the formation of soliton and soliton train in an attractive BEC, where the essential features of the dynamics have been well explained within the mean-field Gross-Pitaevskii model by neglecting molecule formation [36]. A subsequent study including the effect of molecule formation [37] has not essentially changed the conclusions of [36]. Hence this pioneering study on the formation of soliton and soliton trains in a DFFM of different atoms using mean-field hydrodynamic equations with the neglect of molecule formation is expected to explain the essential features of the dynamics. However, it would be of interest to include the effect of molecule formation on the DFFM solitons in a future study.

In section 2 we present our mean-field-hydrodynamic model and its reduction to a quasi-one-dimensional form in a cigar-shaped geometry. In section 3 we show that bright solitons can appear in this model through modulational instability of a constant amplitude solution. In section 4 we perform a variational analysis of the mean-field equations. Numerical results for isolated bright solitons are presented in section 5 and are compared with variational results. Then we study the generation of a train of solitons by modulational instability. Finally, we present a summary in section 6.

2. Nonlinear Model

We use a simplified mean-field-hydrodynamic Lagrangian for a DFG used successfully to study a DBFM [14,20,23]. To develop a set of time-dependent mean-field-hydrodynamic equations for the interacting DFFM, we use the following Lagrangian density [14,20]

$$\mathcal{L} = g_{12}n_1n_2 + \sum_{j=1}^2 \frac{i}{2}\hbar \left[\psi_j \frac{\partial \psi_j^*}{\partial t} - \psi_j^* \frac{\partial \psi_j}{\partial t} \right] + \quad (3)$$

$$+ \sum_{j=1}^2 \left(\frac{\hbar^2 |\nabla_{\mathbf{r}} \psi_j|^2}{6m_j} + V_j(\mathbf{r})n_j + \frac{3}{5}A_j n_j^{5/3} \right),$$

where $j = 1, 2$ represents the two components, ψ_j the probability amplitude, $n_j = |\psi_j|^2$ the probability density, $*$ denotes complex conjugate, m_j the mass, $A_j = \hbar^2(6\pi^2)^{2/3}/(2m_i)$, the interspecies coupling $g_{12} = 2\pi\hbar^2 a_{12}/m_R$ with $m_R = m_1 m_2 / (m_1 + m_2)$ the reduced mass, and a_{12} the interspecies fermion-fermion scattering length. The number of fermionic atoms N_j is given by $\int d\mathbf{r} n_j(\mathbf{r}) = N_j$. The trap potential with axial symmetry is taken as $V_j(\mathbf{r}) = \frac{1}{2}3m_j\omega^2(\rho^2 + \nu^2 z^2)$ where ω and $\nu\omega$ are the angular frequencies in the radial (ρ) and axial (z) directions with ν the anisotropy. The $\nu \rightarrow 0$ limit corresponds to a cigar-shaped geometry and allows a reduction of the three-dimensional equations to a quasi-one-dimensional form appropriate for freely moving solitons. The interaction between identical intra-species fermions in spin-polarized state is highly suppressed due to Pauli blocking terms $3A_j n_j^{5/3}/5$ and has been neglected in (3). The kinetic energy terms $\hbar^2 |\nabla_{\mathbf{r}} \psi_j|^2 / (6m_j)$ in (3) contribute little to this problem compared to the dominating Pauli-blocking terms. However, its inclusion leads to an analytic solution for the probability density everywhere [20].

With the Lagrangian density (3), the following Euler-Lagrange equations:

$$\frac{d}{dt} \frac{\partial \mathcal{L}}{\partial \frac{\partial \psi_j^*}{\partial t}} + \sum_{k=1}^3 \frac{d}{dx_k} \frac{\partial \mathcal{L}}{\partial \frac{\partial \psi_j^*}{\partial x_k}} = \frac{\partial \mathcal{L}}{\partial \psi_j^*}, \quad (4)$$

with $x_k, k = 1, 2, 3$ being the three space components, become

$$\left[i\hbar \frac{\partial}{\partial t} + \frac{\hbar^2 \nabla_{\mathbf{r}}^2}{6m_j} - V_j - A_j n_j^{2/3} - g_{12} n_k \right] \psi_j = 0, \quad (5)$$

where $j \neq k = 1, 2$. This is a time-dependent version of a similar time-independent hydrodynamic model for fermions [13]. For large n_j , both lead to [13, 14] the Thomas-Fermi result [3] $n_j = [(\mu_j - V_j)/A_j]^{3/2}$ with μ_j the chemical potential. They yield identical results for time-independent stationary states. However, the present time-dependent model can be used in the study of nonequilibrium dynamics, as in the study of soliton trains.

For $\nu = 0$, (5) can be reduced to an effective one-dimensional form by considering solutions of the type $\psi_j(\mathbf{r}, t) = \sqrt{N_j} \phi_j(z, t) \psi_j^{(0)}(\rho)$ where

$$|\psi_j^{(0)}(\rho)|^2 \equiv \frac{m\omega}{\pi\hbar} \exp\left(-\frac{m\omega\rho^2}{\hbar}\right), \quad (6)$$

with $m = 3m_j$ corresponds to the ground state wave function in the radial trap alone in the absence of nonlinear interactions. Here to have an algebraic simplification we have taken the masses of two types of fermions to be equal ($m_1 = m_2$). These wave functions satisfy

$$-\frac{\hbar^2}{2m} \nabla_{\rho}^2 \psi_j^{(0)} + \frac{1}{2} m\omega^2 \rho^2 \psi_j^{(0)} = \hbar\omega \psi_j^{(0)}, \quad (7)$$

with normalization $2\pi \int_0^{\infty} |\psi_j^{(0)}(\rho)|^2 \rho d\rho = 1$. Now the dynamics is carried by $\phi_j(z, t)$ and the radial dependence is frozen in the ground state $\psi_j^{(0)}(\rho)$. In the quasi-one-dimensional cigar-shaped geometry the linear fermionic probability densities are given by $|\phi_j(z, t)|^2$.

Averaging over the radial mode $\psi_i^{(0)}(\rho)$, i.e., multiplying (5) by $\psi_i^{(0)*}(\rho)$ and integrating over ρ , we obtain the following one-dimensional dynamical equations [25]:

$$\left[i\hbar \frac{\partial}{\partial t} + \frac{\hbar^2}{2m} \frac{\partial^2}{\partial z^2} - F_{jj} |\phi_j|^{4/3} - F_{jk} |\phi_k|^2 \right] \phi_j(z, t) = 0, \quad (8)$$

where

$$F_{jk} = g_{12} N_k \frac{\int_0^{\infty} |\psi_j^{(0)}|^2 |\psi_k^{(0)}|^2 \rho d\rho}{\int_0^{\infty} |\psi_j^{(0)}|^2 \rho d\rho} = g_{12} \frac{N_k m\omega}{2\pi\hbar},$$

$$F_{jj} = A_j N_j^{2/3} \frac{\int_0^{\infty} |\psi_j^{(0)}|^{2+4/3} \rho d\rho}{\int_0^{\infty} |\psi_j^{(0)}|^2 \rho d\rho} = \frac{3A_j}{5} \left[\frac{N_j m\omega}{\pi\hbar} \right]^{2/3}.$$

In (8) the normalization is given by $\int_{-\infty}^{\infty} |\phi_j(z, t)|^2 dz = 1$. In these equations we have set the anisotropy parameter $\nu = 0$ to remove the axial trap and thus to generate axially-free quasi-one-dimensional solitons.

To reduce three-dimensional equations (8) to a dimensionless form, following [20], we consider variables $\tau = t\omega/2$, $y = z/l$, $\varphi_i = \sqrt{l}\phi_i$, with $l = \sqrt{\hbar/(\omega m)}$, while (8) becomes

$$\left[i \frac{\partial}{\partial \tau} + \frac{\partial^2}{\partial y^2} - N_{jj} |\varphi_j|^{4/3} + N_{jk} |\varphi_k|^2 \right] \varphi_j(y, \tau) = 0, \quad (9)$$

where $N_{jj} = 9(6\pi N_j)^{2/3}/5$, and $N_{jk} = 12|a_{12}|N_k/l$. Here we employ a negative a_{12} corresponding to attraction, and $\int_{-\infty}^{\infty} |\varphi_j(y, \tau)|^2 dy = 1$. In (9) a sufficiently strong attractive fermion-fermion coupling $N_{jk}|\varphi_k|^2$ ($j \neq k$) can overcome the Pauli repulsion $N_{jj}|\varphi_j|^{4/3}$ and form bright solitons.

For the usual Gross-Pitaevskii with the cubic nonlinearity, the reduction of the full three-dimensional equation to its one-dimensional counterpart was performed, in different forms, by many authors [38]. The nonlinearity with 4/3 power in (9) was obtained starting from a similar nonlinearity in a three-dimensional DFG. A strict one-dimensional (two-dimensional) DFG will give rise to a quintic (cubic) nonlinearity. Whatever be the nonlinearity in the intraspecies fermions, bright fermionic solitons will be generated, provided that the interspecies attraction is strong enough to overcome the intraspecies repulsion due to Pauli blocking. However, in this paper we shall consider only the Pauli-blocking nonlinearity with the 4/3 power as in (9).

The two coupled equations (9) could be simplified for $N_1 = N_2 = N$, while $\varphi_1 = \varphi_2 \equiv \varphi$, and these equations reduce to the following single equation

$$\left[i \frac{\partial}{\partial \tau} + \frac{\partial^2}{\partial y^2} - \beta |\varphi|^{4/3} + \gamma |\varphi|^2 \right] \varphi(y, \tau) = 0, \quad (10)$$

where $\beta = N_{11} = N_{22}$ and $\gamma = N_{12} = N_{21}$. Equation (10) maintains the essential features of (9), e.g., a quadratic nonlinear attraction and a Pauli blocking repulsion. The one-dimensional equation (10) is quite similar in structure to the NLS equation (1) apart for the Pauli-blocking repulsive term β . For a small β and large γ the solitons of (1) survive in (10). However, they disappear in the opposite limit of large β and small γ .

3. Modulational Instability

3.1. Symmetric Case ($N_1 = N_2$)

We find that (10) allows a constant-amplitude solution which exhibits modulational instability leading to a modulation of the solution. We perform a stability analysis of this solution and study the possibility of generation of solitons by modulational instability in the symmetric case. We consider the constant-amplitude solution [16]

$$\varphi_0 = A_0 \exp(i\delta) \equiv A_0 \exp[i(\gamma A_0^2 \tau - \beta A_0^{4/3} \tau)] \quad (11)$$

of (10), where A_0 is the constant amplitude and δ a phase. The time evolution of solution (11) maintains the constant amplitude A_0 but acquires an amplitude-dependent phase.

Now we study if this solution is stable against small perturbations by performing a linear stability analysis.

We consider a small perturbation of the constant-amplitude solution (11) given by:

$$\varphi = (A_0 + A) \exp(i\delta), \quad (12)$$

where $A = A(y, \tau)$ is the small perturbation. Substituting the perturbed solution (12) in (10), and for small perturbations retaining only the linear terms in A we get

$$i \frac{\partial A}{\partial \tau} + \frac{\partial^2 A}{\partial y^2} - \frac{2}{3} \beta A_0^{4/3} (A + A^*) + \gamma A_0^2 (A + A^*) = 0. \quad (13)$$

We consider the complex plane-wave perturbation

$$A(y, \tau) = \mathcal{A}_1 \cos(K\tau - \Omega y) + i \mathcal{A}_2 \sin(K\tau - \Omega y) \quad (14)$$

in (13), where \mathcal{A}_1 and \mathcal{A}_2 are the amplitudes of the real and imaginary parts, respectively, and K is a frequency parameter and Ω a wave number. Then separating the real and imaginary parts we get

$$- \mathcal{A}_1 K = \mathcal{A}_2 \Omega^2, \quad (15)$$

$$- \mathcal{A}_2 K = \mathcal{A}_1 \Omega^2 - 2\gamma A_0^2 \mathcal{A}_1 + \frac{4}{3} \beta A_0^{4/3} \mathcal{A}_1, \quad (16)$$

and eliminating \mathcal{A}_1 and \mathcal{A}_2 we obtain the dispersion relation

$$K = \pm \Omega \left[\Omega^2 - (2\gamma A_0^2 - \frac{4}{3} \beta A_0^{4/3}) \right]^{1/2}. \quad (17)$$

The constant-amplitude solution (11) is stable if perturbations at any wave number Ω do not grow with time. This is true as long as frequency K is real. From (17) we find that K remains real for any Ω provided that $2\gamma A_0^2 < 4\beta A_0^{4/3}/3$ or $\gamma A_0^{2/3} < 2\beta/3$. However, K can become imaginary for $\gamma A_0^{2/3} > 2\beta/3$ and the plane-wave perturbations can grow exponentially with time τ . This is the domain of modulational instability of a constant-intensity solution [16]. The perturbation then grows exponentially with the intensity given by the growth rate or the modulational instability gain $g(\Omega)$ defined by

$$g(\Omega) \equiv 2\Im(K) = 2|\Omega| \left[2\gamma A_0^2 - \frac{4}{3} \beta A_0^{4/3} - \Omega^2 \right]^{1/2}, \quad (18)$$

where \Im denotes imaginary part. The presence of modulational instability is closely connected with the appearance of a bright soliton [16]. Localized bright solitons are possible only when the constant-amplitude solution is unstable.

3.2. Asymmetric Case ($N_1 \neq N_2$)

Now we consider the possibility of modulational instability of a similar constant-intensity solution in coupled equations (9). We consider the constant-amplitude solutions

$$\varphi_{j0} = A_{j0} \exp(i\delta_j) \equiv A_{j0} \exp[i\tau(N_{jk}A_{j0}^2 - N_{jj}A_{j0}^{4/3})],$$

of (9), where A_{j0} is the amplitude and δ_j a phase for component j . The constant-amplitude solution develops an amplitude dependent phase on time evolution. We consider a small perturbation $A_j \exp(i\delta_j)$ to these solutions via

$$\varphi_j = (A_{j0} + A_j) \exp(i\delta_j), \quad (19)$$

where $A_j = A_j(y, \tau)$. Substituting this perturbed solution in (9), and for small perturbations retaining only the linear terms in A_j we get

$$\begin{aligned} i \frac{\partial A_j}{\partial \tau} + \frac{\partial^2 A_j}{\partial y^2} - \frac{2}{3} N_{jj} A_{j0}^{4/3} (A_j + A_j^*) + \\ + N_{jk} A_{k0} A_{j0} (A_k + A_k^*) = 0, \quad j \neq k. \end{aligned} \quad (20)$$

We consider the complex plane-wave perturbation

$$A_j(y, \tau) = \mathcal{A}_{j1} \cos(K\tau - \Omega y) + i \mathcal{A}_{j2} \sin(K\tau - \Omega y) \quad (21)$$

in (20) for $j = 1, 2$, where \mathcal{A}_{j1} and \mathcal{A}_{j2} are the amplitudes for the real and imaginary parts, respectively, and K and Ω are frequency and wave numbers. Then separating the real and imaginary parts we get

$$- \mathcal{A}_{11} K = \mathcal{A}_{12} \Omega^2 \quad (22)$$

$$- \mathcal{A}_{12} K = \mathcal{A}_{11} \Omega^2 - 2N_{12} A_{10} A_{20} \mathcal{A}_{21} + \frac{4}{3} N_{11} A_{10}^{4/3} \mathcal{A}_{11}, \quad (23)$$

for $j = 1$, and

$$- \mathcal{A}_{21} K = \mathcal{A}_{22} \Omega^2 \quad (24)$$

$$- \mathcal{A}_{22} K = \mathcal{A}_{21} \Omega^2 - 2N_{21} A_{10} A_{20} \mathcal{A}_{11} + \frac{4}{3} N_{22} A_{20}^{4/3} \mathcal{A}_{21}, \quad (25)$$

for $j = 2$. Eliminating \mathcal{A}_{12} between (22) and (23) we obtain

$$\mathcal{A}_{11} [K^2 - \Omega^2 (\Omega^2 + 4N_{11} A_{10}^{4/3})] = 2\mathcal{A}_{21} N_{12} A_{10} A_{20} \Omega^2, \quad (26)$$

and eliminating \mathcal{A}_{22} between (24) and (25) we obtain

$$\mathcal{A}_{21} [K^2 - \Omega^2 (\Omega^2 + 4N_{22} A_{20}^{4/3})] = 2\mathcal{A}_{11} N_{21} A_{10} A_{20} \Omega^2. \quad (27)$$

Eliminating \mathcal{A}_{11} and \mathcal{A}_{21} from (26) and (27), finally, we obtain the following dispersion relation

$$\begin{aligned} K^2 = \pm \Omega \left[\left(\Omega^2 + \frac{2}{3} N_{11} A_{10}^{4/3} + \frac{2}{3} N_{22} A_{20}^{4/3} \right) \pm \right. \\ \left. \pm \left\{ \frac{4}{9} \left(N_{11} A_{10}^{4/3} - N_{22} A_{20}^{4/3} \right)^2 + 4N_{12} N_{21} A_{10}^2 A_{20}^2 \right\}^{1/2} \right]^{1/2}. \end{aligned} \quad (28)$$

For stability of the plane-wave perturbation, K has to be real. For any Ω this happens for

$$\begin{aligned} & \left(N_{11}A_{10}^{4/3} + N_{22}A_{20}^{4/3} \right)^2 \\ & > \left(N_{11}A_{10}^{4/3} - N_{22}A_{20}^{4/3} \right)^2 + 9N_{12}N_{21}A_{10}^2A_{20}^2, \end{aligned}$$

or for $N_{12}N_{21}A_{10}^{2/3}A_{20}^{2/3} < 4N_{11}N_{22}/9$. However, for $N_{12}N_{21}A_{10}^{2/3}A_{20}^{2/3} > 4N_{11}N_{22}/9$ [39], K can become imaginary and the plane-wave perturbation can grow exponentially with time. This is the domain of modulational instability of a constant-intensity solution signalling the possibility of coupled fermionic bright soliton to appear. In the symmetric case $N_1 = N_2$ and $A_{10} = A_{20} = A_0$, consequently, $N_{11} = N_{22} = \beta$ and $N_{12} = N_{21} = \gamma$ and we recover the condition of modulational instability $\gamma A_0^{2/3} > 2\beta/3$ derived in section 3.1.

4. Variational Analysis

4.1. Symmetric Case ($N_1 = N_2$)

Next we present a variational analysis of (10) based on the Gaussian trial wave function [40]

$$\varphi_v(y, \tau) = A \exp \left[-\frac{y^2}{2R^2(\tau)} + \frac{i}{2}b(\tau)y^2 + ic(\tau) \right], \quad (29)$$

where A is the amplitude, R is the width, b the chirp, and c the phase. The Lagrangian density for (10) is the one-term version of (3), e.g.,

$$\mathcal{L} = \frac{i}{2}\hbar \left[\varphi \frac{\partial \varphi^*}{\partial t} - \varphi^* \frac{\partial \varphi}{\partial t} \right] + \left| \frac{\partial \varphi}{\partial y} \right|^2 - \frac{1}{2}\gamma n^2 + \frac{3}{5}\beta n^{5/3},$$

which is evaluated with this trial function and the effective Lagrangian $L = \int_{-\infty}^{\infty} \mathcal{L}(\varphi_v) dy$ becomes

$$\begin{aligned} L = & \frac{A^2 R \sqrt{\pi}}{2} \left(\frac{6\sqrt{3}}{5\sqrt{5}} \beta A^{4/3} + 2\dot{c} - \frac{\gamma}{\sqrt{2}} A^2 + \right. \\ & \left. + \frac{R^2 \dot{b}}{2} + \frac{1}{R^2} + b^2 R^2 \right), \end{aligned} \quad (30)$$

where the overhead dot denotes time derivative. The variational Lagrange equations

$$\frac{d}{dt} \frac{\partial L}{\partial \dot{q}} = \frac{\partial L}{\partial q}, \quad (31)$$

where q stands for c , A , R and b can then be written as

$$A^2 R = \frac{1}{\sqrt{\pi}} = \text{constant}. \quad (32)$$

$$\dot{b} = -\frac{2}{R^4} - 2b^2 + 2\sqrt{2}\gamma\frac{A^2}{R^2} - 4\frac{\sqrt{3}}{\sqrt{5}}\beta\frac{A^{4/3}}{R^2} - \frac{4\dot{c}}{R^2}, \quad (33)$$

$$3\dot{b} = \frac{2}{R^4} - 6b^2 + \sqrt{2}\gamma\frac{A^2}{R^2} - \frac{12}{5}\frac{\sqrt{3}}{\sqrt{5}}\beta\frac{A^{4/3}}{R^2} - \frac{4\dot{c}}{R^2}, \quad (34)$$

$$\dot{R} = 2Rb. \quad (35)$$

The constant in (32) is fixed by the normalization condition. Eliminating \dot{c} from (33) and (34) we obtain

$$\dot{b} = \frac{2}{R^4} - 2b^2 - \frac{1}{\sqrt{2}}\gamma\frac{A^2}{R^2} + \frac{4}{5}\frac{\sqrt{3}}{\sqrt{5}}\beta\frac{A^{4/3}}{R^2}. \quad (36)$$

The use of (32), (35) and (36) leads to the following differential equation for the width R :

$$\frac{d^2R}{d\tau^2} = \left(\frac{4}{R^3} - \frac{\gamma}{R^2}\sqrt{\frac{2}{\pi}} + \frac{1}{R^{5/3}}\frac{8\beta\sqrt{3}}{5\pi^{1/3}\sqrt{5}} \right) \quad (37)$$

$$= -\frac{d}{dR} \left[\frac{2}{R^2} - \frac{\gamma}{R}\sqrt{\frac{2}{\pi}} + \frac{1}{R^{2/3}}\frac{12\beta\sqrt{3}}{5\pi^{1/3}\sqrt{5}} \right]. \quad (38)$$

The quantity in the square bracket is the effective potential of the equation of motion. Small oscillation around a stable configuration is possible when there is a minimum in this potential. The variational result for width R follows by setting the right hand side of (37) to zero corresponding to a minimum in this effective potential, from which the variational profile for the soliton can be obtained [40].

4.2. Asymmetric Case ($N_1 \neq N_2$)

The above variational analysis can be extended to the asymmetric case. However, the algebra becomes quite involved if we take a general variational trial wave function with chirp and phase parameters. As we are interested mostly in the density profiles, we consider the following normalized Gaussian trial wave function for fermion component j of (9)

$$\varphi_{vj} = \sqrt{\frac{1}{R_j(\tau)\sqrt{\pi}}} \exp\left[-\frac{y^2}{2R_j^2(\tau)}\right], \quad j = 1, 2. \quad (39)$$

Using essentially the Lagrangian density (3) in this case we obtain the following effective Lagrangian

$$L = -\frac{1}{\sqrt{\pi}}\frac{N_{jk}N_j}{\sqrt{R_1^2 + R_2^2}} + \sum_{j=1}^2 \frac{N_j}{2} \left(\frac{6\sqrt{3}}{5\sqrt{5}\pi^{1/3}}\frac{N_{jj}}{R_j^{2/3}} + \frac{1}{R_j^2} \right),$$

with $j \neq k = 1, 2$. The variational Lagrange equations (31) for R_1 and R_2 now become

$$\frac{4}{R_j^3} - \frac{4N_{jk}}{\sqrt{\pi}}\frac{R_j}{(R_1^2 + R_2^2)^{3/2}} + \frac{8\sqrt{3}}{5\sqrt{5}\pi^{1/3}}\frac{N_{jj}}{R_j^{5/3}} = 0. \quad (40)$$

Equations (40) can be solved for variational widths R_j and consequently the variational profile of the wave functions obtained from (39). When $N_1 = N_2$, in (40) $N_{jj} = \beta$,

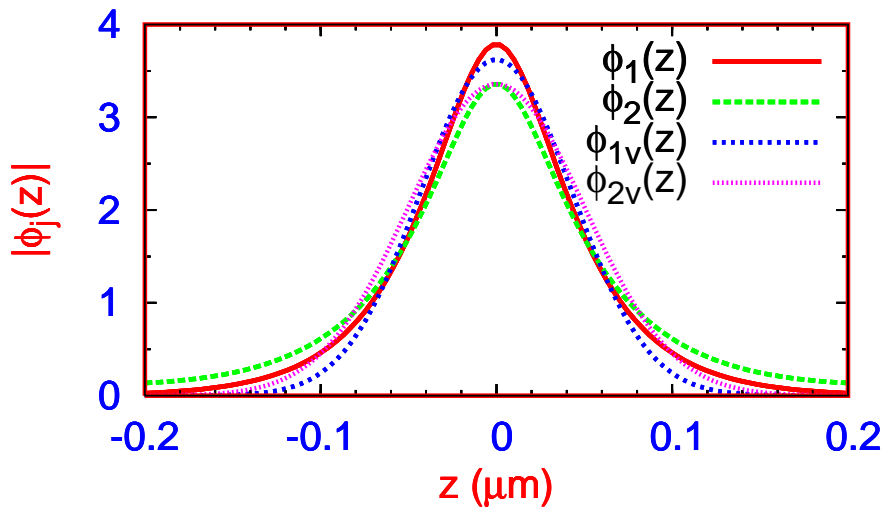


Figure 1. The solitons $|\phi_j(z)|$ of (9) vs. z for $N_1 = 40$, $N_2 = 60$, $a_{12} = -300$ nm, while $N_{11} \approx 149$, $N_{12} = 216$, $N_{21} = 144$, and $N_{22} \approx 195$. The corresponding variational solutions $\phi_{jv}(z)$ calculated from the coupled equations (40) are also shown.

$N_{jk} = N_{kj} = \gamma$ and $R_1 = R_2 = R$; and in this case (40) yields the same variational widths as from the result obtained in the symmetric case in section 4.1 given by (37); e. g.,

$$\frac{4}{R^3} - \frac{\gamma}{R^2} \sqrt{\frac{2}{\pi}} + \frac{1}{R^{5/3}} \frac{8\beta\sqrt{3}}{5\pi^{1/3}\sqrt{5}} = 0. \quad (41)$$

5. Numerical Results

We solve (9) for bright solitons numerically using a time-iteration method based on the Crank-Nicholson discretization scheme [41]. We discretize the coupled partial differential equations (9) using time step 0.0002 and space step 0.015 in the domain $-8 < y < 8$. The second derivative in y is discretized by a three-point finite-difference rule and the first derivative in τ by a two-point finite-difference rule. We perform a time evolution of (9) introducing an harmonic oscillator potential y^2 in it and setting the nonlinear terms to zero, and starting with the eigenfunction of the harmonic oscillator problem: $\varphi_i(y, \tau) = \pi^{-1/4} \exp(-y^2/2) \exp(-i\tau)$. The extra harmonic oscillator potential, set equal to zero in the end, only aids in starting the time evolution with an exact analytic form. With this initial solution we perform time evolution of (9). During the time evolution the nonlinear terms are switched on slowly and the harmonic oscillator potential is switched off slowly and the time evolution continued to obtain the final converged solutions. In addition to solving the coupled equations (9), we also solved the single equation (10) in the symmetric case: $N_1 = N_2$. For given values of N_1 and N_2 , solitons can be obtained for $|a_{12}|$ above a certain value. In the coupled-channel case solitons are easily obtained for a smaller $|a_{12}|$ when N_1 and N_2 are not very different from each other.

In our numerical study we take $l = 1 \mu\text{m}$ and consider a DFFM consisting of two electronic states of ^{40}K atoms. This corresponds to a radial trap of frequency $\omega = \hbar/(l^2m) \approx 2\pi \times 83 \text{ Hz}$. Consequently, the unit of time is $2/\omega \approx 4 \text{ ms}$. For another fermionic atom the ω value gets changed accordingly for $l = 1 \mu\text{m}$.

5.1. Single Soliton

From a solution of coupled equations (9) we find that these equations permit solitonic solutions provided that $|a_{12}|$ is larger than a certain threshold value consistent with the analysis of section 3. First we solve (9) for $N_1 = 40$, $N_2 = 60$, and $a_{12} = -300 \text{ nm}$. In this case no solitons are allowed for $a_{12} = -290 \text{ nm}$. The solitonic solution suddenly appears as $|a_{12}|$ increases past 290 nm . The solitons in this case are shown in figure 1, where we also plot the variational solutions of coupled equations (40). In this case the nonlinearity parameters are $N_{11} \approx 149$, $N_{12} = 216$, $N_{21} = 144$, and $N_{22} \approx 195$. Substituting these values of the nonlinearities in (40) and solving we obtain the variational widths $R_1 \approx 0.043$ and $R_2 \approx 0.050$. From (29) and (32) we then obtain the variational soliton profiles $|\phi_{v1}(z)| \approx 3.62 \exp(-270z^2)$ and $|\phi_{v2}(z)| \approx 3.36 \exp(-200z^2)$. From figure 1 we find that the variational results agree well with the numerical solutions of the coupled equations. In this case we also found the variational result in the symmetric case ($N_1 = N_2 = 50$) using (41), which lies close to the above two variational solutions.

To test the robustness of these solitons we inflicted different perturbations on them and studied the resultant dynamics numerically. First, after the formation of the solitons of figure 1 with $N_1 = 40$ and $N_2 = 60$ we suddenly changed the particle numbers to $N_1 = 60$ and $N_2 = 40$ at time $t = 100 \text{ ms}$. This corresponds to a sudden change of nonlinearities from $N_{11} \approx 149$, $N_{12} = 216$, $N_{21} = 144$, and $N_{22} \approx 195$ to $N_{11} \approx 195$, $N_{12} = 144$, $N_{21} = 216$, and $N_{22} \approx 149$. The resultant dynamics is shown in figures 2a and 2b. Due to the sudden change in nonlinearities, the fermionic bright solitons are set into stable non-periodic small-amplitude breathing oscillation. This demonstrates the robustness of the solitons.

After the formation of the solitons of figure 1 with $N_1 = 40$ and $N_2 = 60$ we suddenly changed the interspecies scattering length a_{12} from -300 nm to -330 nm at time $t = 100 \text{ ms}$. This can be realized by manipulating a background magnetic field near a fermion-fermion Feshbach resonance [26] This corresponds to a sudden change of nonlinearities from $N_{11} \approx 149$, $N_{12} = 216$, $N_{21} = 144$, and $N_{22} \approx 195$ to $N_{11} \approx 149$, $N_{12} \approx 238$, $N_{21} \approx 158$, and $N_{22} \approx 195$. Due to the sudden change in nonlinearities, the fermionic bright solitons are set into stable non-periodic small-amplitude breathing oscillation. Instead of plotting the soliton profile in this case we plot the root mean square (rms) size of the solitons in figure 3 which demonstrates the stable nonperiodic breathing oscillation. We also (i) gave a small displacement between the centers of these solitons and (ii) suddenly changed $\phi_1 \rightarrow 1.1 \times \phi_1$ and $\phi_2 \rightarrow 1.1 \times \phi_2$. In both cases after oscillation and dissipation the solitons continue stable propagation which shows their robust nature.

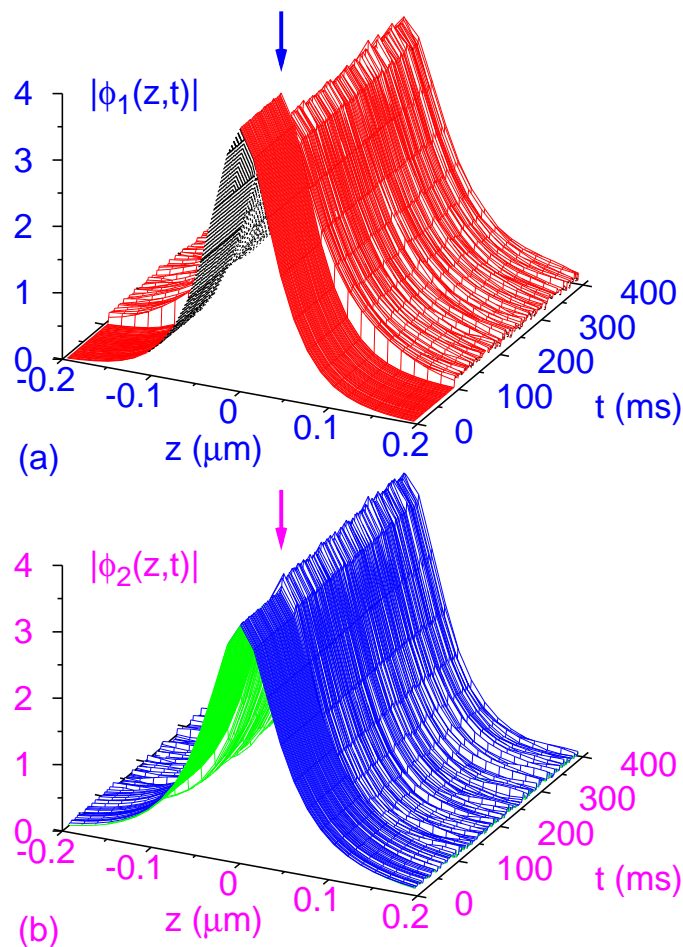


Figure 2. The propagation of fermionic solitons (a) $|\phi_1(z,t)|$ and (b) $|\phi_2(z,t)|$ of figure 1 vs. z and t for $N_1 = 40$ and $N_2 = 60$. At $t = 100$ ms (marked by arrows) the bright solitons are set into small breathing oscillation by suddenly changing the fermion numbers to $N_1 = 60$ and $N_2 = 40$.

5.2. Soliton Train

During the time evolution of (9) if the nonlinearities are changed by a small amount or changed slowly, usually one gets a single stable soliton when the final nonlinearities are appropriate. However, if the interspecies attraction is increased suddenly by a large amount by jumping a_{12} from a positive (repulsive) value to a large negative (attractive) value, a soliton train is formed as in the experiment with BEC [1] because of modulational instability [42].

To illustrate the formation of soliton train in a fermion-fermion mixture in numerical simulation, we consider the solution of (9) for $N_1 = N_2 = 40$ and $a_{12} = -300$ nm with an added axial harmonic trap y^2 corresponding to nonlinearities $N_{jj} \approx 149$ and $N_{jk} \approx 144, j \neq k = 1, 2$. After the formation of the solitons in the axial trap we suddenly jump the scattering length to -400 nm, corresponding to off-diagonal nonlinearities $N_{jk} = 192$, and also switch off the harmonic trap at time $t = 0$. Although

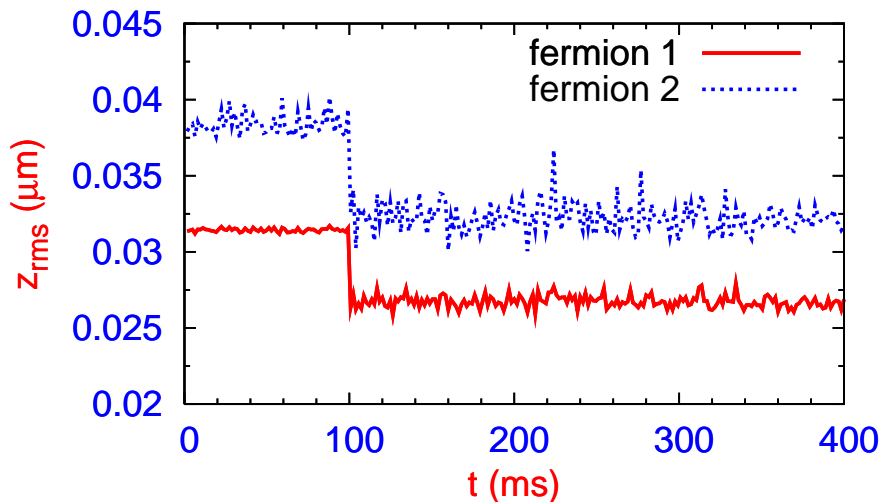


Figure 3. The rms sizes of the solitons $|\phi_1(z, t)|$ and $|\phi_2(z, t)|$ of figure 1 vs. t . At $t = 100$ ms the solitons of figure 1 are set into small breathing oscillation by suddenly changing a_{12} from -300 nm to -330 nm.

the initial value of scattering length ($a_{12} = -300$ nm) in this case corresponds to an interatomic attraction, because of strong Pauli-blocking repulsion the effective fermion-fermion interaction is repulsive in this case. However, the final value of scattering length ($a_{12} = -400$ nm) corresponds to a stronger interatomic attraction which can overcome the Pauli repulsion so that an effective fermion-fermion attraction emerges in this case which might allow the formation of soliton(s). In our numerical simulation we find that this is indeed the case. Upon a jump of the scattering length to $a_{12} = -400$ nm, we find that after some initial noise and dissipation the time evolution of (9) generates a single stable bright soliton as shown in figure 4a.

However, more solitons in the form of a soliton train can be formed for a larger jump in the scattering length. In figure 4b, from the same initial state in figure 4a we consider a larger jump of a_{12} to -570 nm corresponding to off-diagonal nonlinearities $N_{jk} \approx 274$. The final value of scattering length ($a_{12} = -570$ nm) in this case corresponds to a stronger interatomic attraction than considered in figure 4a which might allow the formation of soliton trains. This is verified in numerical simulation. Upon a jump of the scattering length to $a_{12} = -570$ nm, from $a_{12} = -300$ nm, we find that after some initial noise and dissipation the time evolution of (9) generates three slowly receding bright solitons as shown in figure 4b. More solitons can be generated when the jump in the scattering length a_{12} or off-diagonal nonlinearities is larger.

In figure 4c we show the generation of five receding solitons of each component upon a sudden jump of the scattering length a_{12} to -750 nm from the initial state of figure 4a. This corresponds to a jump of the off-diagonal nonlinearities to $N_{jk} \approx 360$. The formation of soliton trains from a stable initial state is due to modulational instability [16]. The sudden jump in the off-diagonal nonlinearities could be effected by

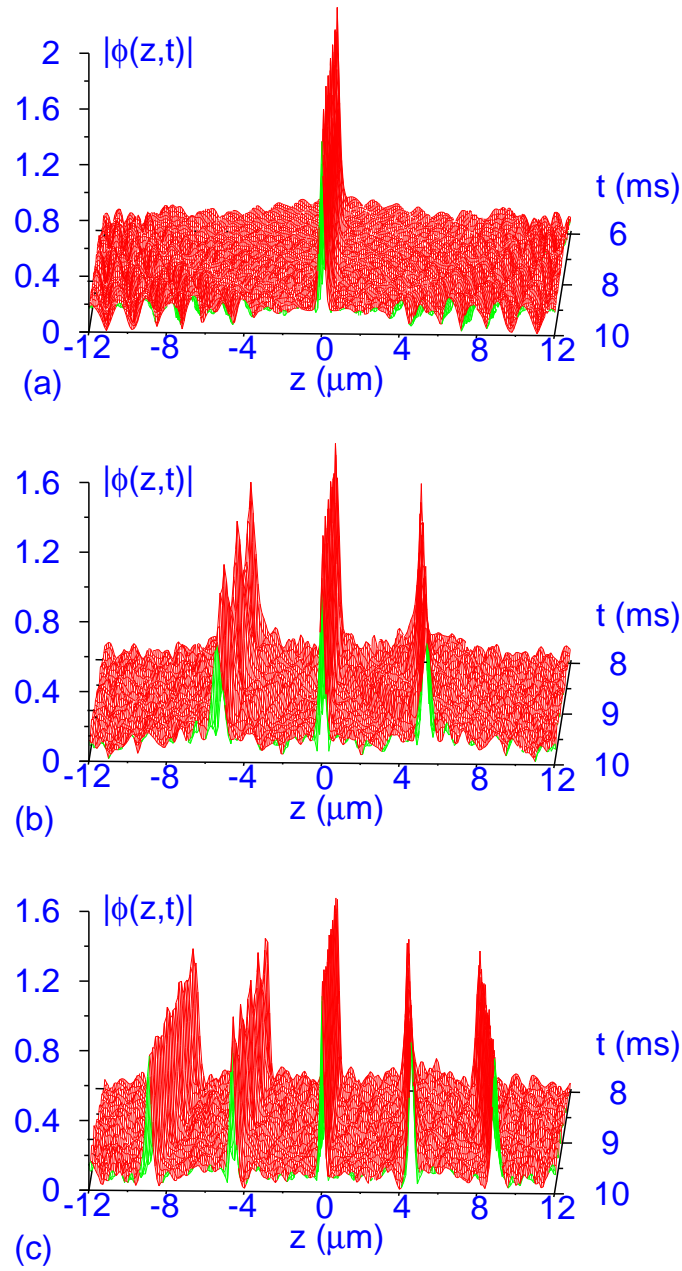


Figure 4. Soliton trains of one, three and five solitons formed for $N_1 = N_2 = 40$ upon removing the harmonic trap y^2 and jumping the nonlinearities at $t = 0$ from $N_{jj} \approx 149, N_{jk} \approx 144, k \neq j = 1, 2$ to (a) $N_{jj} \approx 149, N_{jk} \approx 192$, (b) $N_{jj} \approx 149, N_{jk} \approx 274$, and to (c) $N_{jj} \approx 149, N_{jk} \approx 360$, respectively, corresponding to a jump in scattering length a_{12} from -300 nm to -400 nm, -570 nm, and -750 nm. For this purpose we solved the coupled equations (9).

a jump in the interspecies scattering length a_{12} obtained by manipulating a background magnetic field near a Feshbach resonance [26].

6. Summary

We used a coupled mean-field-hydrodynamic model for a DFFM to study the formation of bright solitons and soliton trains in a quasi-one-dimensional geometry by numerical and variational methods. We find that an attractive interspecies interaction can overcome the Pauli repulsion and form fermionic bright solitons in a DFFM. This is similar to the formation of bright solitons in a coupled boson-boson [21] and boson-fermion [19, 20] mixtures supported by interspecies interaction. We show by a linear stability analysis that when the interspecies attraction is larger than a threshold value, bright solitons can be formed due to modulational instability of a constant-amplitude solution of the nonlinear equations describing the DFFM.

The stability of these solitons is demonstrated numerically through their sustained breathing oscillation initiated by a sudden small perturbation. We also illustrate the creation of soliton trains upon a sudden large jump in interspecies attraction by manipulating a background magnetic field near a Feshbach resonance [26] resulting in a sudden jump in the off-diagonal nonlinearities. This jump transforms an effectively repulsive DFFM into an effectively attractive one, responsible for the formation of a soliton train due to modulational instability. Bright solitons and soliton trains have been created experimentally in attractive BECs in the presence of a radial trap only without any axial trap [1] in a similar fashion by transforming a repulsive BEC into an attractive one. In view of this, fermionic bright solitons and trains could be created in laboratory in a DFFM in a quasi-one-dimensional configuration.

Here we used a set of mean-field equations for the DFFM. A proper treatment of a DFG or DFFM should be done using a fully antisymmetrized many-body Slater determinant wave function [11, 19, 43] as in the case of scattering involving many electrons [44]. However, in view of the success of a fermionic mean-field model in studies of collapse [14], bright [20] and dark [23] soliton in a DBFM and of mixing and demixing in a DFFM [25], we do not believe that the present study on bright solitons in a DFFM to be so peculiar as to have no general validity.

Acknowledgments

The work is supported in part by the CNPq and FAPESP of Brazil.

References

- [1] Strecker K E *et al.* 2002 *Nature* **417** 150
- [2] Khaykovich L *et al.* 2002 *Science* **296** 1290
- [3] Dalfovo F, Giorgini S, Pitaevskii L P and Stringari S 1999 *Rev. Mod. Phys.* **71** 463
Yukalov V I 2004 *Laser Phys. Lett.* **1** 435

- Yukalov V I and Yukalova E R *Laser Phys. Lett.* 2004 **1** 50
 Yukalov V I and Girardeau M D *Laser Phys. Lett.* 2005 **2** 375.
 Abdullaev F K, Gammal A, Kamchatnov A M and Tomio L 2005 *Int. J. Mod. Phys. B* **19** 3415
- [4] DeMarco B and Jin D S 1999 *Science* **285** 1703
- [5] O'Hara K M, Hemmer S L, Gehm M E, Granade S R and Thomas J E 2002 *Science* **298** 2179
- [6] Schreck F, Khaykovich L, Corwin K L, Ferrari G, Bourdel T, Cubizolles J and Salomon C 2001 *Phys. Rev. Lett.* **87** 080403
 Truscott A G, Strecker K E, McAlexander W I, Partridge G B and Hulet R G 2001 *Science* **291** 2570
- [7] Hadzibabic Z, Stan C A, Dieckmann K, Gupta S, Zwierlein M W, Gorlitz A and Ketterle W 2002 *Phys. Rev. Lett.* **88** 160401
- [8] Modugno G, Roati G, Riboli F, Ferlaino F, Brecha R J and Inguscio M 2002 *Science* **297** 2240
 Ospelkaus C, Ospelkaus S, Sengstock K and Bongs K 2006 *Phys. Rev. Lett.* **96** 020401
- [9] Roati G, Riboli F, Modugno G and Inguscio M 2002 *Phys. Rev. Lett.* **89** 150403
- [10] Strecker K E, Partridge G B and Hulet R G 2003 *Phys. Rev. Lett.* **91** 080406
 Hadzibabic Z, Gupta S, Stan C A, Schunck C H, Zwierlein M W, Dieckmann K and Ketterle W 2003 *Phys. Rev. Lett.* **91** 160401
- [11] Molmer K 1998 *Phys. Rev. Lett.* **80** 1804
- [12] Roth R 2002 *Phys. Rev. A* **66** 013614
 Roth R and Feldmeier H 2001 *J. Phys. B: At. Mol. Opt. Phys.* **34** 4629
 Roth R and Feldmeier H 2002 *Phys. Rev. A* **65** 021603R
 Miyakawa T, Suzuki T and Yabu H 2001 *Phys. Rev. A* **64** 033611
 Liu X-J and Hu H 2003 *Phys. Rev. A* **67** 023613
 Vichi L, Amoruso M, Minguzzi A, Stringari S and Tosi M P 2000 *Eur. Phys. J. D* **11** 335
 Amoruso A, Meccoli I, Minguzzi A and Tosi M P 2000 *Eur. Phys. J. D* **8** 361
 Modugno M, Ferlaino F, Riboli F, Roati G, Modugno G and Inguscio M 2003 *Phys. Rev. A* **68** 043626
 Jezek D M *et al.* 2004 *Phys. Rev. A* **70** 043630
- [13] Capuzzi P, Minguzzi A and Tosi M P 2004 *Phys. Rev. A* **69** 053615
 Capuzzi P, Minguzzi A and Tosi M P 2003 *Phys. Rev. A* **67** 053605
- [14] Adhikari S K 2004 *Phys. Rev. A* **70** 043617
- [15] Pérez-García V M, Michinel H and Herrero H 1998 *Phys. Rev. A* **57** 3837
 Adhikari S K 2003 *New J. Phys.* **5** 137
- [16] Kivshar Y S and Agrawal G P 2003 *Optical Solitons - From Fibers to Photonic Crystals* (San Diego, Academic)
- [17] Abdullaev F K, Caputo J G, Kraenkel R A and Malomed B A 2003 *Phys. Rev. A* **67** 013605
 Saito H and Ueda M 2003 *Phys. Rev. Lett.* **64** 040403
 Montesinos G D, Pérez-García V M, Michinel H 2004 *Phys. Rev. Lett.* **92** 133901
 Adhikari S K *Phys. Rev. A* **69** 063613
 Adhikari S K *Phys. Rev. E* **71** 016611
- [18] Alfimov G L, Konotop V V and Salerno M 2002 *Europhys. Lett.* **58** 7
 Louis P J Y, Ostrovskaya E A, Savage C M and Kivshar Y S 2003 *Phys. Rev. A* **67** 013602
 Abdullaev F K and Salerno M 2005 *Phys. Rev. A* **72** 033617
 Maytevarunyo T and Malomed B A 2006 *Phys. Rev. A* **74** 033616
- [19] Karpiuk T *et al.* 2004 *Phys. Rev. Lett.* **93** 100401
 Karpiuk T, Brewczyk M and Rzaewski K 2006 *Phys. Rev. A* **73** 053602
- [20] Adhikari S K 2005 *Phys. Rev. A* **72** 053608
 Adhikari S K 2006 *Laser Phys. Lett.* **3** 553
- [21] Pérez-García V M and Beitia J B 2005 *Phys. Rev. A* **72** 033620
 Adhikari S K 2005 *Phys. Lett. A* **346** 179
- [22] Adhikari S K 2002 *Phys. Rev. A* **66** 013611

- Adhikari S K 2001 *Phys. Rev. A* **63** 043611
- [23] Adhikari S K 2005 *J. Phys. B: At. Mol. Opt. Phys.* **38** 3607
- [24] Adhikari S K 2006 *J. Low Temp. Phys.* **143** 267
Adhikari S K 2006 *Laser Phys. Lett.* **3** 605
- [25] Adhikari S K 2006 *Phys. Rev. A* **73** 043619
Adhikari S K and Malomed B A 2006 *Phys. Rev. A* **74** 053620
- [26] O'Hara K M *et al.* 2002 *Phys. Rev. A* **66** 041401(R)
Dieckmann K *et al.* 2002 *Phys. Rev. Lett.* **89** 203201
Loftus T *et al.* 2002 *Phys. Rev. Lett.* **88** 173201
Regal C A, Greiner M and Jin D S 2004 *Phys. Rev. Lett.* **92** 083201
- [27] Gehm M E, Hemmer S L, Granade S R, O'Hara K M and Thomas J E 2003 *Phys. Rev. A* **68** 011401(R)
- [28] Kokkelmans S J J M F, Milstein J N, Chiofalo M L, Walser R and Holland M J 2002 *Phys. Rev. A* **65** 053617
- [29] Heiselberg H 2001 *Phys. Rev. A* **63** 043606
- [30] Hulet R G 2006 private communication. I thank Dr. Hulet for a discussion, which clarified this point, suggesting the enhanced possibility of the formation of soliton train in a DFFM of different atoms.
- [31] Chin C, Bartenstein M, Altmeyer A, Riedl S, Jochim S, Denschlag J H and Grimm R 2004 *Science* **305** 1128
Partridge G B, Li W H, Kamar R I, Liao Y A and Hulet R G 2006 *Science* **311** 503
- [32] Bardeen J, Cooper L N and Schrieffer J R 1957 *Phys. Rev.* **108** 1175
- [33] Eagles D M 1969 *Phys. Rev.* **186** 456
Leggett A J 1980 *J. Phys. (Paris) Colloq.* **41** C7-19
Casas M *et al* 1994 *Phys. Rev. B* **50** 15945
- [34] Strecker K E, Partridge G B and Hulet R G 2003 *Phys. Rev. Lett.* **91** 080406
- [35] Adhikari S K 2006 *New J. Phys.* **8** 258
- [36] Al Khawaja U, Stoof H T C, Hulet R G, Strecker K E and Partridge G B 2002 *Phys. Rev. Lett.* **89** 200404
- [37] Salasnich L, Parola A and Reatto L 2003 *Phys. Rev. Lett.* **91** 080405
- [38] Salasnich L, Parola A and Reatto L 2002 *Phys. Rev. A* **65** 043614
Salasnich L, Parola A and Reatto L 2002 *Phys. Rev. A* **66** 043603
Salasnich L and Malomed B A 2006 *Phys. Rev. A* **74** 053610
Khaykovich L and Malomed B A 2006 *Phys. Rev. A* **74** 023607
- [39] Kourakis I *et al.* 2005 *Eur. Phys. J. B* **46** 381
- [40] Anderson D 1983 *Phys. Rev. A* **27** 3135
Pérez-García V M, Michinel H, Cirac J I, Lewenstein M and Zoller P 1997 *Phys. Rev. A* **56** 1424
Stoof H T C 1997 *J. Stat. Phys.* **87** 1353
Malomed B A 2002 in *Progress in Optics, vol. 43, p. 71, ed. by Wolf E* (Amsterdam, North-Holland)
- [41] Muruganandam P and Adhikari S K 2003 *J. Phys. B: At. Mol. Opt. Phys.* **36** 2501
Adhikari S K 2000 *Phys. Rev. E* **62** 2937
Adhikari S K 2002 *Phys. Rev. A* **66** 013611
- [42] Tai K, Hasegawa A and Tomita A 1986 *Phys. Rev. Lett.* **56** 135
- [43] Salerno M 2005 *Phys. Rev. A* **72** 063602
- [44] Biswas P K and Adhikari S K 2000 *J. Phys. B: At. Mol. Opt. Phys.* **33** 1575
Biswas P K and Adhikari S K 1998 *J. Phys. B: At. Mol. Opt. Phys.* **31** L315
Tomio L and Adhikari S K 1980 *Phys. Rev. C* **22** 28
Adhikari S K and Ghosh A 1997 *J. Phys. A: Math. Gen.* **30** 6553
Adhikari S K 1979 *Phys. Rev. C* **19** 1729